http://dx.doi.org/10.5012/bkcs.2013.34.12.3738

# Theoretical Study of the Reaction Mechanism for $SiF_2$ Radical with HNCO

**Li-Jie Hou,* Bo-Wan Wu, Chao Kong, Yan-Xia Han, Dong-Ping Chen, and Li-Guo Gao†**

*School of Chemistry & Chemical Engineering, Longdong University, Qingyang 745000, China*
**E-mail: 200hlj@163.com*
*†School of Chemistry & Chemical Engineering, Yulin University, Lanzhou 730070, China*
*Received July 3, 2013, Accepted September 23, 2013*

The reaction mechanism of $SiF_2$ radical with HNCO has been investigated by the B3LYP method of density functional theory(DFT), while the geometries and harmonic vibration frequencies of reactants, intermediates, transition states and products have been calculated at the B3LYP/6-311++G** level. To obtain more precise energy result, stationary point energies were calculated at the CCSD(T)/6-311++G**//B3LYP/6-311++G** level. $SiF_2$+HNCO→IM3→TS5→IM4→TS6→$OSiF_2CNH$(P3) was the main channel with low potential energy, $OSiF_2CNH$ was the main product. The analyses for the combining interaction between $SiF_2$ radical and HNCO with the atom-in-molecules theory (AIM) have been performed.

**Key Words :** $SiF_2$ radical, Isocyanic acid, Reaction mechanism, AIM

## Introduction

Isocyanic acid, HCNO, a major thermal decomposition product of cyanuric acid, is an important in $NO_x$ pollutant emissions from fossil-fuel combustion.[1-3] In recent years, many experimental investigations on HNCO have been performed.[4-15] Some studies have reported the photolysis reactions[4-8] and the polymerization pathways of HNCO.[15] Theoretical study of the reaction mechanism for small molecules with HNCO is a hot topic.[10-14,17-29] Liu *et al*.[30] have report the reaction between HNCO and CX (X=F, Cl, Br) free radicals. The renewed public interest of the $CF_2$ radical as the intermediate of many fluorocarbon combination reactions is continuing. Li *et al*.[31] have report the quantum chemical and topological study on the C-C bond insertion and cycloaddition reaction mechanism of $CX_2$. Apparently, the correlative reactions about HNCO are very important. As important intermediates of many silicon fluoride reactions, it is important theoretical and practical significance to research silicon fluorine radical. In this report, we use the density functional theory (DFT) to explore the reaction mechanism of $SiF_2$ radical with HNCO, we hope our work provide some valuable fundamental insights into HNCO and $SiF_2$ radical.

## Calculation Methods

All calculations have been performed with the Gaussian03 package.[32] Geometry optimization at the DFT-B3LYP/6-311++G** level[33-36] is used to obtain geometries of reactants, intermediates, transition states and products. The harmonic vibration frequencies are also obtained at the corresponding level to characterize the stationary points as local minima or first-order saddle points. The intrinsic reaction coordinate (IRC) calculation is used to track minimum energy paths from transition structures to the corresponding local minima. To obtain more precise energy result, stationary point energies are calculated at the CCSD(T)/6-311++G**//B3LYP/6-311++G** level of theory.

## Results and Discussion

Calculations show that the ground state of $SiF_2$ radical is the singlet state, its energy is lower than the triplet 269.6 kJ/mol, so only the reaction of $SiF_2$ radicals with isocyanic acid on singlet is discussed in this article. The NBO calculation results show that precursor complex IM1 and IM6 form when the $SiF_2$ radical approaches HNCO through interaction of an empty *p* orbital of Si atom with lone pair electrons of N atom. C-N bond is weakened, then NH abstraction reaction starts. In IM3, C-O bond is weakened because lone pair of electrons of O atom and $\sigma^*$(C-O) in HNCO interact with empty *p* orbital of Si atom in $SiF_2$ radical. O atom abstraction reaction is occurred from IM3 and IM9. In IM5, N-H bond is weakened because $\sigma^*$(C-N) in HNCO interacts with empty *p* orbital of Si atom in $SiF_2$ radical, then absorption H reaction is occurred from IM6. Therefore, the reaction of $SiF_2$ radical with HNCO is complicated and multichannel.

**O-atom Abstraction Channel.** We can see from Figure 1, the Si atom combines with C and O atom of IM3 to form an stable three-membered ringy intermediate IM4 through transition state TS4, TS5 respectively, the formation of the Si-C bond leads to the weakness of O-C bond. IM3 through TS4 formatting IM4, the O-C bond length increases from 0.1304 nm to 0.1448 nm. As displayed in Table 1, the charge density ($\rho(r)$) of the O-C bonding critical points (*BCP*) decreases gradually from 0.4459 to 0.2483, which signifies the bond strength gradually weaken. The value of $\nabla^2\rho(r)$ is gradually reduced as the reaction proceeds, which indicates the covalency of the O-C bond is more stronger. IM3 through the transition state TS5 formatting IM4, the O-C bond length increases from 0.1249 nm to 0.1448 nm, and it

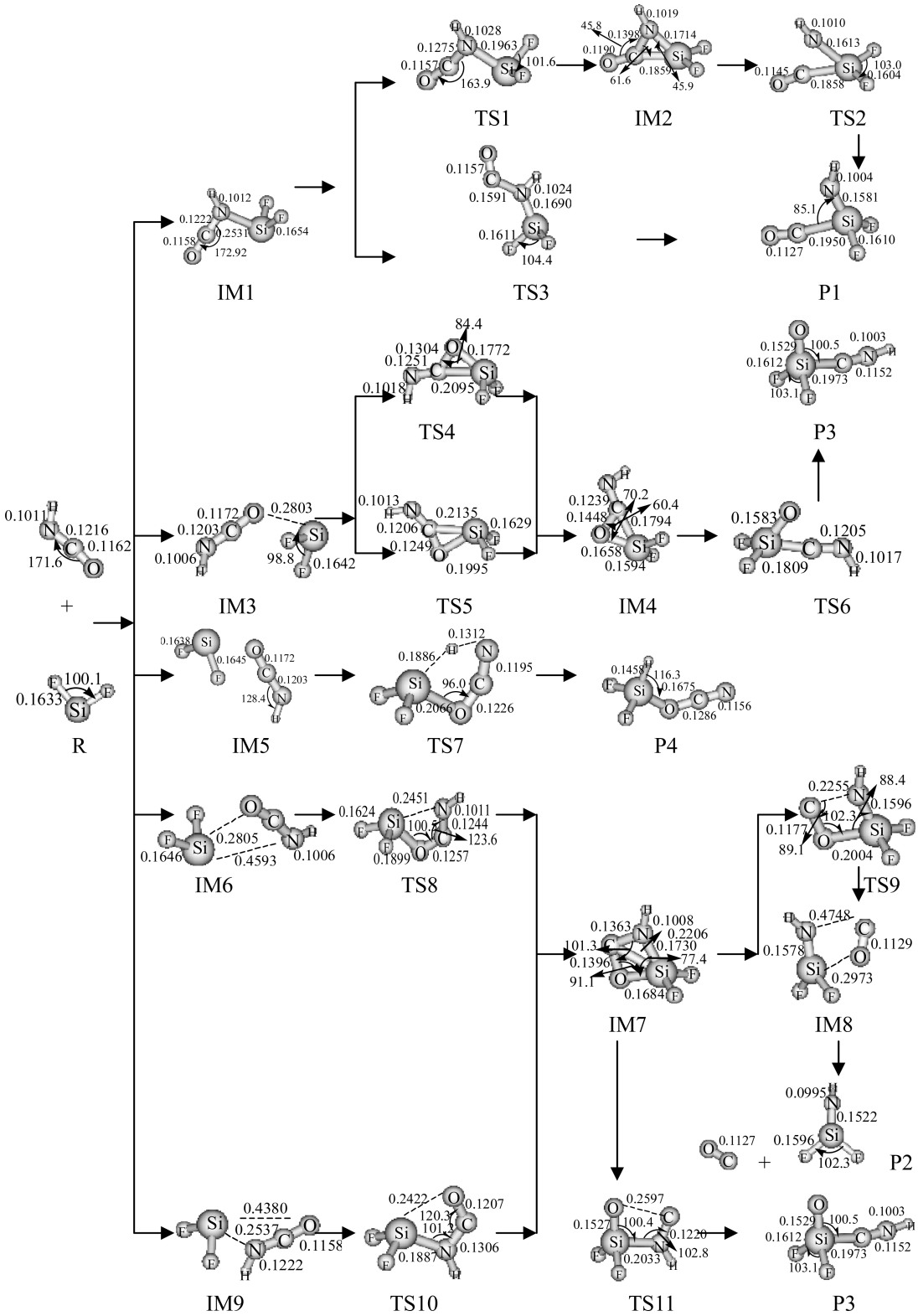


**Figure 1.** Optimized geometries of various species in reaction (bond lengths in nm and bond angles in degree).

stretches gradually. The Si-O bond length decreases gradually from 0.1658 nm to 0.1529 nm, subsequently, IM4 forms a more stable product 3 ($OSiF_2CNH$)(P3) through transition state TS6. The $\rho(r)$ of the Si-O bonding critical points (*BCP*) increases gradually from 0.1342 to 0.1807, which indicates the Si-O bond strength is gradually enhanced. The ovality ε is gradually reduced, which indicates the π bonding characteristic of the Si-O bond is weakened. The O-C bond length gradually stretches until the bond disconnects to generate P3.

**Table 1.** Electron density topological characteristics of main chemical bonds of optimized geometries during the $SiF_2$ reacting with HNCO in O-atom and H abstraction channel

| Bond Specie | Si-N | | | Bond Specie | Si-O | | |
|---|---|---|---|---|---|---|---|
| | $\rho(r_c)$ | $\nabla^2\rho\ (r_c)$ | ε | | $\rho(r_c)$ | $\nabla^2\rho\ (r_c)$ | ε |
| IM7 | 0.1283 | 0.5645 | 0.0020 | IM4 | 0. 0141 | 0. 0348 | 0. 0100 |
| IM9 | 0.0287 | 0.0383 | 0.0291 | TS4 | 0. 1052 | 0. 4329 | 0. 3153 |
| TS10 | 0.0100 | 0.1961 | 0.0253 | IM5 | 0. 1342 | 0. 8674 | 0. 1334 |
| TS11 | 0.1567 | 0.6543 | 0.0017 | TS6 | 0. 1606 | 1. 1780 | 0. 0071 |
| | | Si-H | | TS7 | 0.0654 | 0.0091 | 0.1026 |
| TS7 | 0.7290 | -0.0632 | 0.0296 | P4 | 0.1208 | 0.7811 | 0.0108 |
| P4 | 0.1341 | 0.2130 | 0.0074 | IM7 | 0.1329 | 0.7247 | 0.0145 |
| | | C-O | | TS10 | 0.0419 | 0.5762 | 0.1625 |
| IM4 | 0. 4459 | -0.0596 | 0. 0060 | TS11 | 0.1453 | 0.7734 | 0.0256 |
| TS4 | 0. 3221 | -0.1028 | 0. 2486 | P3 | 0.1807 | 1.4630 | 0.0163 |
| TS5 | 0. 3824 | -0.5277 | 0. 0549 | | | | |
| IM5 | 0. 2483 | -0.4234 | 0. 1196 | | | | |

As shown in Figure 2, the IM3 forms IM4 through TS4 with energy barrier of 266.9 kJ/mol and through TS5 with energy barrier of 47.0 kJ/mol. Obviously, the process of IM3→TS5→IM4 is easy to occur and it is advantageous in the kinetics. IM4 changes into P3 through TS6 with energy barrier of 22.7 kJ/mol. This step is favorable kinetically. The whole reaction is exothermic 76.6 kJ/mol, which is thermodynamically favorable too. Therefore, O atom abstraction through TS5 channel is the major reaction channel.

As displayed in Figure 2, the $SiF_2$ radical collides with HNCO to generate reactant intermediate IM9, which is barrier-free exothermic process of 60.6 kJ/mol. IM9 through transition state TS10 to form a stable four-membered ring intermediate IM7 with energy of 110.3 kJ/mol. The intermediate IM8 forms P3 through a transition state TS11 with energy of 118.5 kJ/mol. We can see from Figure 1, the Si-N bond length decreases from 0.2537 nm in IM9 to 0.1887 nm in TS10 to 0.1730 nm in IM7, the bond is to be formed, but it increases from 0.2033 nm in TS11 to 0.3109 nm in P3, clearly, the Si-N bond is to cleave. The Si -O bond length decreases from 0.4830 nm in IM9 to 0.2422 nm in TS10 to 0.1684 nm in IM7 to 0.1527 nm in TS11 to 0.1529 nm in P3. then the Si-O bond is to be formed. Compared with the pathway above, this two-step reaction barrier is higher. Therefore, O-atom abstraction through four-membered ring channel is the minor reaction pathway.

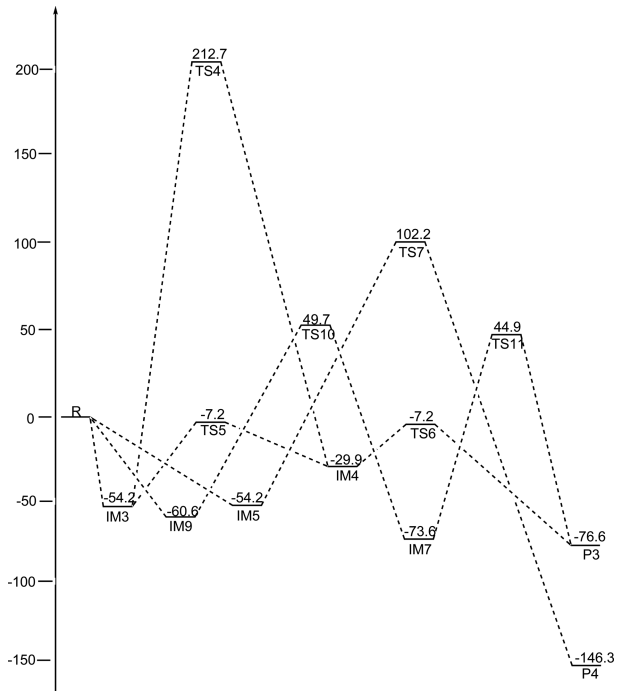


**Figure 2.** Schematic map of energy levels of O and H abstraction channels (relative energies in kJ/mol).

**NH Abstraction Channel.** HNCO collides with the $SiF_2$ radical to form an intermediate IM1, the energy decreases by 61.6 kJ/mol. The C atom combines with Si atom of IM1 to form an stable three-membered ring intermediate IM2 through a transition state TS1, the potential energy is 71.0 kJ/mol. After that, IM2 forms an product 1($SiF_2$NHCO)(P1) through a transition state TS2, the bond length of C-N increases from 0.1222 nm in IM1 to 0.1275 nm in TS1 to 0.1398 nm in IM2 to 0.1958 nm in TS2, clearly, the C-N bond is to cleave. But N-Si bond length decreases from 0.2531 nm in IM1 to 0.1963 nm in TS1 to 0.1714 nm in IM2 to 0.1613 nm in TS2 to 0.1581 nm in P1, clearly, the C-Si bond is to be formed. As can be seen in support information, the entire reaction process, the $\rho(r)$ of N-Si bonding critical points (*BCP*) is gradually increased from 0.0289 in IM1 to 0.1682 in P1, which indicates that the bond strength is gradually enhanced until the bond generates. The $\nabla^2\rho(r)$ is gradually increased, which indicates the ionicity of N-Si bond is enhanced. the $\rho(r)$ of C-N bonding critical points (*BCP*) is gradually reduced from 0.4186 to 0.2266, which indicates that the bond strength is weakened, until the C-N bond rupture in P1. The $\nabla^2\rho(r)$ gradually increases from negative to positive, the ionicity of C-N bond is dominated and strengthened gradually, which illustrates the process of broken bond vividly, finally the P1 is formed.

IM1 can form P1 through transition state TS3 with energy barrier of 162.0 kJ/mol too. On TS3, the Si-N bond length is shorter about 0.0840 nm and the N-C bond is longer about 0.0369 nm than IM3. Finally, the N-C bond dissociates to the P1. The $\rho(r)$ of Si-N bonding critical points (*BCP*) gradually increased in the whole reaction, but the C-N bond is the opposite, which show vividly the process of the C-N bond cleavage and NH migration to the Si atom. The potential energy of the two pathways above are higher than O atom abstraction through TS5 pathway. Consequently, two reaction channels above are not the main reaction channel.

The formation of intermediate IM6 is barrier-free exothermic process of 54.2 kJ/mol. IM6 through transition state TS8 forms a stable four-membered ring intermediate IM7 with energy of 132.4 kJ/mol. Subsequently, IM7 dissociates to IM8 through transition state TS9. IM8 decomposes into $SiF_2NH$ and CO (product 2) (P2) with energy of 143.9 kJ/mol. The Si-N bond length decreases from 0.4593 nm in IM6 to 0.1522 nm in P2, but the C-O bond length increases from 0.1203 nm in IM9 to 0.4748 nm in IM8. Clearly, the Si-N bond is to be formed, the C-N bond is to cleave. The potential energy of this two-step reaction is high and the reaction is endothermic. No matter in the dynamics and thermodynamics, the reaction is unfavorable. Therefore, the channel of NH abstraction through four-membered ring is the minor reaction pathway.

**Absorption H Channel.** HNCO collides with the $SiF_2$ radical to form the intermediate IM5, then IM5 forms the product 4($HSiF_2OCN$)(P4) through transition state TS7. As shown in Figure 1, The bond length of Si-O and Si-H decrease to 0.2066 nm and 0.1886 nm from IM5 to TS7, to 0.1675 nm and 0.1458 nm from TS7 to P4 respectively. Clearly, the Si-O and Si-H bond are to be form, absorption H reaction is performed. Table 1 lists, the $\rho(r)$ of Si-O and Si-H bonding critical points (*BCP*) is gradually increased, which indicate that two bonds strength are enhanced, until two bonds generate. the $\nabla^2\rho(r)$ of Si-H bond gradually increases from negative to positive, the ionicity nature of the bond strengthen, the ovality is gradually reduced to 0.0074, which signifies the Si-H bond is an typical σ bond.

As shown in Figure 2, the process of the IM5 changing into P4 through TS7 with energy barrier of 156.4 kJ/mol is not easy to occur because the barrier is more higher. The reaction is exothermic 146.3 kJ/mol. Therefore, this pathway is not the main reaction pathway.

## Conclusions

In this study, the B3LYP method of density functional theory is employed to study the reaction mechanism for $SiF_2$ radical with HNCO and seven feasible pathways are investigated in the singlet state. The changes of bond length and the low activation energy show all that the reaction pathways are feasible. Furthermore, the topological properties of the chemical bonds of various configurations verify these reaction pathways through AIM.

Comparing the activation energy of seven reaction pathways, it can be concluded that O atom abstraction through transition state TS5 channel is the energetically favorable to occur because the potential energy is the lowest and the reaction is exothermic. This theoretical study may be useful as a guide to future synthetic efforts and to problems that merit further study by both theory and experiment.

**Acknowledgments.** This work is supported by the Natural Science Foundation of Gansu Province under Grant No. 1208RJZM289.

## References

1. Perry, R. A.; Siebers, D. L. *Nature* **1986**, *324*(6098), 657-658.
2. Miller, J. A.; Bowman, C. T. *Int. J. Chem. Kinet.* **1991**, *23*(4), 289-313.
3. Zyrianov, M.; Droz-Georget, T. *J. Chem. Phys.* **1996**, *105*(18), 8111-8116.
4. Steven, J. E.; Qiang, C.; Morokuma, K. *J. Chem. Phys.* **1998**, *108*(4), 1452-1474.
5. Fang, W. H.; You, X. Z.; Zhen, Y. *Chem. Phys. Lett.* **1995**, *238*, 236-242.
6. Brown, S. S.; Cheatum, C. M.; Fitzwater, D. A. *et al. J. Chem. Phys.* **1996**, *105*(24), 10911-10918.
7. Klossica, J. J.; Lothmann, H. F.; Yamashita, K. *Chem. Phys. Lett.* **1997**, *276*, 325-330.
8. Zyrianov, M.; Droz-Georget, Th.; Reisler, H. *J. Chem. Phys.* **1999**, *110*(4), 2059-2068.
9. Reinhard, S.; Martina, B. *Chem. Phys. Lett.* **2000**, *332*, 611-615.
10. Mertens, J. D.; Kohse-Honghans, K. *et al. Int. J. Chem. Kinet.* **1991**, *23*, 655-658.
11. Raunier, S.; Chiavassa, T.; Marinelli, F. *et al. Chem. Phys. Lett.* **2003**, *368*, 594-600.
12. Xu, Z. F.; Sun, C. C. *J. Phys. Chem. A* **1998**, *102*(7), 1194-1199.
13. Xu, Z. F.; Sun, C. C. *J. Mol. Struct. (Theochem)* **1999**, *459*, 37-46.
14. Raunier, S.; Chiavassa, T.; Allouche, A. *et al. Chem. Phys.* **2003**, *288*(2), 197-210.
15. Geith, J.; Klapotke, T. M. *J. Mol. Struct. (Theochem)* **2001**, *538*(1), 29-39.
16. Xu, Z. F.; Sun, C. C. *J. Mol. Struct. (Theochem)* **1999**, *459*, 37-46.
17. Ji, Y. Q.; Feng, W. L.; Xu, Z. F. *Science in China Series B-Chemistry* **2002**, *32*(2), 172-178.
18. Karl-Martin, H.; Jessica, S.; Claes, T. *et al. Å. Combust. Flame* **2004**, *137*(3), 265-277.
19. Ma, S. Y.; Ji, Y. G.; Liu, R. Z. *Acta Chim. Sin.* **1997**, *55*, 110-116.
20. Zhao, L.; Li, Z. H. *Science in China Series B-Chemistry* **2001**, *31*(2), 123-129.
21. Zhang, X. Z.; Zhen, Z.; Liu, X. H. *Science in China Series B-Chemistry* **2004**, *34*(4), 339-345.
22. Kong, C.; Han, Y. X.; Chen, D. P. *J. At. Mol. Phys.* **2011**, *28*(5), 823-829.
23. Hou, L. J.; Kong, C.; Han, Y. X.; Chen, D. P. *et al. J. At. Mol. Phys.* **2012**, *29*(6), 753-764.
24. Liu, J. L.; Shang, J.; Wang, P. Y. *et al. Acta Phys. Chim. Sin.* **2006**, *22*(8), 921-925.
25. Zha, D.; Li, L. C.; Zhu, Y. Q. *et al. Acta Chim. Sin.* **2005**, *63*(19), 1782-1788.
26. Shang, J.; Zha, D.; Li, L. C. *et al. Acta Chim. Sin.* **2006**, *64*(9), 923-929.
27. Li, L. C.; Liu, J. L.; Shang, J. *Chin. J. Chem. Physics* **2006**, *19*(5), 451-456.
28. Li, L. C.; Z, Y.; Zha, D. *Int. J. Quantum Chem.* **2006**, *106*(7), 1672-1682.
29. David, S. Y.; Umstead, M. E.; Lin, M. C. *ACS Symp. Ser.* **1978**, *66*, 128-151.
30. Liu, P. J.; Pan, X. M.; Zhao, M. *Acta Chim. Sin.* **2002**, *60*(11),

1941-1945.
31. Li, Z. F.; Zhu, Y. C.; Li, H. X. *et al. J. At. Mol. Phys.* **2009**, *26*(5), 821-701.
32. Frisch, M. J.; Trucks, G. W.; Schlegel, H. B.; Scuseria, G. E.; Robb, M. A.; Cheeseman, J. R.; Montgomery, J. A., Jr.; Vreven, T.; Kudin, K. N.; Burant, J. C.; Millam, J. M.; Iyengar, S. S.; Tomasi, J.; Barone, V.; Mennucci, B.; Cossi, M.; Scalmani, G.; Rega, N.; Petersson, G. A.; Nakatsuji, H.; Hada, M.; Ehara, M.; Toyota, K.; Fukuda, R.; Hasegawa, J.; Ishida, M.; Nakajima, T.; Honda, Y.; Kitao, O.; Nakai, H.; Klene, M.; Li, X.; Knox, J. E.; Hratchian, H. P.; Cross, J. B.; Adamo, C.; Jaramillo, J.; Gomperts, R.; Stratmann, R. E.; Yazyev, O.; Austin, A. J.; Cammi, R.; Pomelli, C.; Ochterski, J. W.; Ayala, P. Y.; Morokuma, K.; Voth, G. A.; Salvador, P.; Dannenberg, J. J.; Zakrzewski, V. G.; Dapprich, S.; Daniels, A. D.; Strain, M. C.; Farkas, O.; Malick, D. K.; Rabuck, A. D.; Raghavachari, K.; Foresman, J. B.; Ortiz, J. V.; Cui, Q.; Baboul, A. G.; Clifford, S.; Cioslowski, J.; Stefanov, B. B.; Liu, G.; Liashenko, A.; Piskorz, P.; Komaromi, I.; Martin, R. L.; Fox, D. J.; Keith, T.; Al-Laham, M. A.; Peng, C. Y.; Nanayakkara, A.; Challacombe, M.; Gill, P. M. W.; Johnson, B.; Chen, W.; Wong, M. W.; Gonzalez, C.; Pople, J. A. *Gaussian 03*, Revision B.01, Gaussian, Inc., Pittsburgh PA, 2003.
33. Su, M. D.; Chu, S. Y. *J. Am. Chem. Soc.* **1999**, *121*, 4229-4237.
34. Becke, A. D.; Kohn, W.; Parr, R. G. *J. Phys. Chem.* **1996**, *100*, 12974-12980.
35. Becke, A. D. *Phys. Rev. A* **1988**, *38*(6), 3098-3100.
36. Fukui, K. *J. Phys. Chem.* **1970**, *74*, 4161-4163.